Journal of Applied Polymer Science

Preparation, structure, and property of wood flour incorporated polypropylene composites prepared by a solid-state mechanochemical method

Zhihai Niu, Yinghong Chen, Jiabing Feng
State Key Laboratory of Polymer Materials Engineering, Polymer Research Institute of Sichuan University, Chengdu, People's Republic of China
Correspondence to: Y. Chen (E-mail: johnchen@scu.edu.cn)

ABSTRACT: In this article, a solid-state mechanochemical method based on a pan-mill equipment was used to prepare 60 wt % loading of wood flour (WF) incorporated polypropylene (PP) wood–plastic composite (WPC) with good comprehensive performance. The particle size distribution, crystallization, microstructure, and properties of the prepared WPC were accordingly investigated. The results show that under co-effects of the strong shear force field of pan milling and the compatibilization of PP grafted maleic anhydride (PP-g-MAH), the mixture of PP and WF is effectively pulverized and homogeneously mixed. Meanwhile, the WF particles are adequately activated by exposure of their characteristic functional groups, which is beneficial to the interfacial mechanochemical reaction. PP-g-MAH and PP prove to be in situ grafted onto WF particles surface during pan milling, thus resulting in the substantial enhancement in both the dispersion of the added WF fillers in PP matrix and the interfacial bonding. The mechanochemical effects of pan milling could also remarkably promote the heterogeneous nucleation effect of WF particles on PP crystallization and influence the dynamic mechanical behavior of composite. Compared with the unmilled and uncompatibilized composite, the milled and compatibilized WPC material possesses greatly enhanced mechanical performance and shows good application prospects. © 2015 Wiley Periodicals, Inc. J. Appl. Polym. Sci. **2016**, *133*, 43108.

KEYWORDS: cellulose and other wood products; composites; mechanical properties; morphology; polyolefins

Received 13 August 2015; accepted 29 October 2015
DOI: 10.1002/app.43108

INTRODUCTION

The wood flour (WF) is a kind of lignocellulosic material containing various cellulose fibers such as cellulose, hemicelluloses, lignin, etc.[1] and hence could be an environmentally renewable resource.[2] The lignocellulosic material possesses many advantages such as light weight, high mechanical strength, easy availability, no abrasion to processing equipment, low cost, and biodegradability (the most attractive property).[3] As a result, the WF was often used as a filler to be composited with the thermoplastic polymer to manufacture the wood–plastic composite (WPC)[4] as a replacement for the solid wood material with high cost. Because the WPCs combine the advantages of wood and plastic, e.g., the good dimensional stability and the good mechanical strength of the former and the excellent processability and the recyclable property of the latter, they have been broadly applied in many fields such as building, furniture, garden, packaging, car industries, etc. In addition, the raw materials for preparation of WPC could be the waste plant fibers (WF, rice husk, crop stalk, etc.) and the waste plastic. So, this is undoubtedly beneficial to reduction in the environmental pollution, which is partly from the burning of a large amount of agricultural wastes and waste plastic materials. Obviously, WPC is an eco-friendly green product[5,6] deserved to be further developed.

However, there are challenges in preparation of WPC materials with a good comprehensive performance, which are reflected in the following three aspects: the difficult dispersion of WF in polymer matrix, the poor interfacial combination of WF with polymer matrix, and the difficult processing of WF incorporated polymer system. Generally, for most WPCs to be potentially applied in industry, a WF loading of 30–60 wt %[7–9] is required to render the prepared WPCs high strength and low cost. Obviously, for such a WPC system with a high WF loading, realization of the good dispersion of WF and also the processing and molding of the mixture is not easy. In addition, there are a large amount of hydrophilic hydroxyl groups on the surface of WF,

Additional Supporting Information may be found in the online version of this article.

which is the essential reason for the poor interfacial adhesion between the WF and the thermoplastic polymer. On the other hand, the hydroxyl groups on the surface of WF would also result in the strong interactions between WF particles, which make the WF very easily agglomerated and hence difficultly dispersed in polymer matrix. Obviously, the poor interfacial compatibility and the bad WF filler dispersion would surely lead to the obvious deterioration in the mechanical properties of the prepared WPC. In order to improve the interfacial compatibility and the WF filler dispersion, various methods[10] were adopted. These strategies include addition of compatibilizer,[11–15] use of coupling agent,[16–20] alkali treatment,[21–24] heat treatment,[25,26] low-temperature plasma treatment[21] and surface grafting copolymerization,[27–29] where the first one is mostly adopted. Lai *et al.*[13] examined the effects of different compatibilizers on the mechanical properties of high-density polyethylene/WF composites. They found that maleated linear low-density and high-density polyethylene gave higher tensile and impact strengths for the composites, whereas maleated polypropylene (PP) only slightly improved the tensile modulus and tensile strength. Tronc *et al.*[1] investigated the blue agave fiber esterification and its use in thermoplastic composite reinforcement. The results showed that superficial modification improved the impact resistance and produced an enhancement in fiber/HDPE interfacial interaction. Karmarkar *et al.*[3] investigated the effect of a novel compatibilizer with isocyanate functional group (m-TMI-g-PP) on mechanical properties of wood–fiber reinforced PP composites. The addition of the compatibilizer leaded to an almost 45% and 85% increase in the tensile strength and flexural property of composite, respectively. But the addition of wood–fibers resulted in a decrease in elongation at break and impact strength of the composite. It is seen that through introduction of compatibilizer or adoption of surface modification, the corresponding mechanical performance of the prepared WPC is enhanced to different extent. However, the loading of lignocellulosic filler reported in literatures[7–9,11–29] is usually lower than 60 wt % (mostly in the range of 30–50 wt %) and seldom exceeds 60 wt %. Obviously, incorporation of the WF with a loading of 60 wt % or higher is much more attractive for the industry to prepare the WPC with a reduced cost. For this purpose, the improvement in the dispersion of the WF filler and the processability of the mixture of WF filler with polymer is critical, as mentioned before.

This article focuses on the preparation of PP-based WPCs with 60 wt % WF loading. In order to overcome the challenges in preparation of the highly filled PP/WF composite, a solid-state mechanochemical method, also called solid-state shear milling (S^3M) method, developed in the authors' laboratory is used. This technology is based on the authors' self-designed pan-mill equipment,[30] of which the structure is derived from the Chinese traditional stone mill [the structure and image of this equipment can be found in the Supporting Information (Figures S1–S3)]. The key part of this innovative equipment is the inlaid mill pan, whose surface is divided into equal sectors by several bevels; the ridges of the bevels are parallel to the dividing lines. This equipment can be operated at room temperature and can exert a very strong squeezing force in the normal direction and shearing force in both radial and tangential directions on the milled materials in between during milling, functioning like three-dimensional scissors. Based on the smart structure of the pan-mill equipment, it proves to have multifunctions including pulverization, dispersion, mixing and initiation of mechanochemical reaction.[31–35] Because in the authors' previous work,[36] the processing problem of the highly filled WPC system (the WF loading is even up to 80 wt %) has been well resolved, the aim of this work is to realize the good dispersion of WF filler in PP matrix and enhancement of the interfacial compatibility using the S^3M technology and also to prepare the WPC with good comprehensive performance. The influences of pan milling and the introduced compatibilizer polypropylene grafted maleic anhydride (PP-g-MAH) on the pulverization, crystallization, structure and property of the WF/PP system were systematically investigated.

Table I. The Composition of the Wood Plastic Composite System

Composition code	WF (wt %)	PP (wt %)	PP-g-MAH (wt %)
WPC0	60	40	0
WPC3	60	37	3
WPC5	60	35	5
WPC10	60	30	10

EXPERIMENTAL

Materials

Polypropylene (T30s) was purchased from PetroChina Company (Dushanzi, China) in the form of homopolymer pellets (2 mm) with a density of 0.91 g/cm^3 and a melt flow index of 2.0–4.0 g/10 min (230°C/2.160 kg). WF with a particle size of 250 μm was purchased from Qingdao Fumulin New Energy & Equipment Co. (Qingdao, China). Polypropylene grafted maleic anhydride (PP-MAH, CMPP3015) with a graft rate of 1.0% was provided by Bluestar New Material Co. (Chengdu, China).

Preparation of Samples

The dried WF, PP, and PP-g-MAH with formulations shown in Table I were first premixed in a high-speed mixer and then the mixture was fed into the pan mill through the hopper at a rotation speed of 30 rpm. The milled particles were discharged from the edge of the mill pan. Then, the discharged powder was collected for the next milling cycle. The milling was conducted at room temperature and the cooling water was used to remove the heat generated during milling. The milling process was repeated for 20 cycles and every 5 cycles a proper amount of composite powder (co-powder) was taken out for the further experiments. The obtained co-powder was dried at 100°C for 6 h. The dried co-powder was then extruded at 180°C in a TSSJ-25/33 co-rotating twin screw extruder ($\Phi = 25$ mm, $L/D = 33$, Chenguang Research Institute of Chemical Industry, China) with a rotation rate of 120 rpm. The extrudates were cooled in a water bath, cut into pellets and dried at 100°C for 6 h. The dried pellets were then injection molded into various standard test bars at 190°C using a MA1200-SMS-A injection molding machine (Haitian Plastics Machinery, China). For

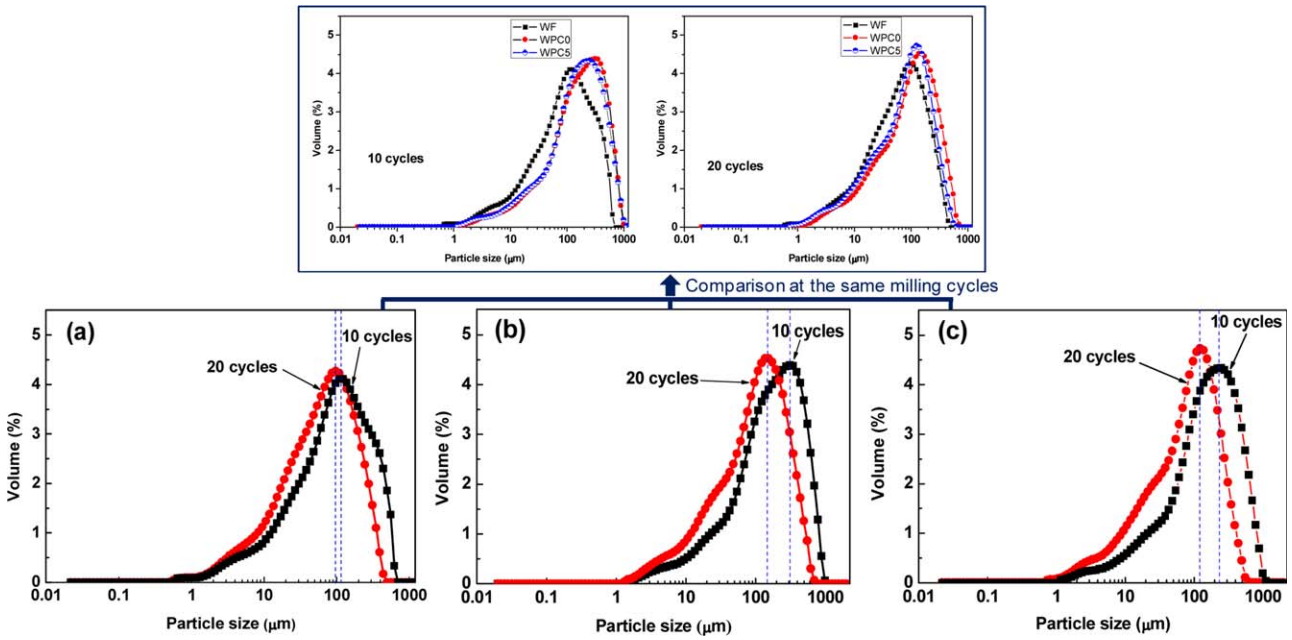

Figure 1. Particle size distribution of (a) pure wood flour, (b) WPC0 and (c) WPC5 co-powders at different milling cycle. [Color figure can be viewed in the online issue, which is available at wileyonlinelibrary.com.]

convenience, the prepared PP/PP-MAH/WF composite with different content of PP-g-MAH was abbreviated as WPC*n*, where *n* is the content of PP-g-MAH multiplied by 100.

Characterization

The Fourier transform infrared spectra (FT-IR) of different samples were recorded on a Nicolet 20SXB Infrared spectrometer in the range of 4000–400 cm^{-1} with a resolution of 4 cm^{-1} over 20 scans. Before measurement, the WPC0 and WPC5 co-powder samples with 20 milling cycles were extracted in a Soxhlet extractor using boiling dimethylbenzene for 72 h to remove the free PP and PP-g-MAH. Particle size and its distribution of co-powder were determined using laser particle size analyzer (Malvern Instruments Co., UK) with alcohol solvent as the dispersing medium and the pump speed was set at 2400 r/min. The crystallization behaviors of pure PP and WPC samples were investigated using a TA Q20 differential scanning calorimeter (DSC) (TA Instruments, USA). Samples with 5–10 mg were heated from 40 to 190°C with a heating rate of 10°C/min and a dynamic nitrogen flow of 50 mL/min. At 190°C, the samples were annealed for 5 min to eliminate the heat history and then cooled to 40°C with the same nitrogen flow rate and a cooling rate of 10°C/min. The corresponding crystallization curves were recorded. The sample crystallinity $X_c = \Delta H/(\Delta H_0 \times \alpha) \times 100\%$, where ΔH is the measured melting enthalpy, α is the weight content of PP in the composite, and ΔH_0 is the melting enthalpy of 100% crystalline PP (208.9 J/g).[37] The dynamic mechanical analysis (DMA) of WPC was performed on a TA Q800 dynamic mechanical thermal analyzer (TA Instruments, USA) in a three-point bending mode at a frequency of 1 Hz. The temperature range was set from −100 to 150°C at a heating rate of 3°C/min. The sample size was 35 × 10 × 4 mm. The morphologies of the co-powder and the fractured surface of injection molded bars of WPC were observed on a JEOL JSM-5900LV scanning electronic microscope (SEM) (JEOL, Japan) with an acceleration voltage of 5 or 20 kV. The specimens were cryogenically fractured in liquid nitrogen. The fractured surfaces were coated with a conductive gold layer before observation. The tensile strength and flexural strength of the WPC sample were measured at ambient temperature using an Instron universal testing machine 4302 (Instron Corporation, UK) with a crosshead speed of 50 mm/min according to ASTM D638 and in a three point loading mode according to ASTM D790, respectively. The notched impact tests were conducted at ambient temperature on a ZBC-4B impact tester (Shenzhen Xinsansi Measurement Technology Co., China) according to ASTM D256 standard. The test result of mechanical property of each sample is the averaged value of five measurements.

RESULTS AND DISCUSSION

Preparation and Characterization of PP/WF co-Powder

Particle Size Analysis. In order to investigate the influence of pan milling and PP-g-MAH addition on the pulverization efficiency of the mixture of PP with WF, the particle size analysis was carried out on pure WF and the WPC co-powders with different milling cycles and different PP-g-MAH content. The results are shown in Figure 1. As can be seen, at the same milling cycles (10 or 20), the particle size of co-powder of WF with polymer (WPC0) is constantly higher than that of pure WF. This indicates that the complex aggregate particles consisting of WF and polymer could be possibly formed through their strong interaction under the very strong shear force field of pan milling. The structure of the complex aggregate particle will be investigated in the following part. In addition, the influence of pan milling on the size reduction of pure WF is obviously smaller than that of its mixture with PP polymer. With increase of milling cycles, relative to pure WF, the particle size distribution of PP/WF and PP/WF/PP-g-MAH co-powder shifts toward

Table II. The Specific Surface Area of Pure Wood Flour and PP/WF Co-powder with Different PP-g-MAH Content at Different Milling Cycles

	Pure wood flour		WPC0 composition		WPC3 composition	
Milling cycles	10	20	10	20	10	20
Specific surface area (m^2/g)	0.26	0.33	0.13	0.20	0.15	0.28

the low-particle-size direction more obviously. This reveals that under the effect of WF as a grinding aid, the mixture of PP with WF is more effectively pulverized where the pulverization of polymer predominates. Comparing Figure 1(c) with Figure 1(b), it is obvious that for the PP-g-MAH contained system (WPC5), the incorporation PP-g-MAH could further decrease the particle size of PP/WF co-powder and with increasing milling cycles to 20, the volume of the particles with the reduced size (the height of particle size distribution peak) obviously increases, indicating that the addition of PP-g-MAH is beneficial to reduction in particle size of PP/WF co-powder. This could be ascribed to the enhanced interaction between PP macromolecular chains and WF due to the introduction of PP-g-MAH. The specific surface area of powder can indirectly reflect its particle size to a certain extent. The smaller the particle size, the greater the specific surface area. The measured specific surface area summarized in Table II further verifies the results of particle size analysis, i.e., the increase of milling cycle results in decrease in particle size. The particle size of PP/WF co-powder is bigger than that of pure WF. The addition of PP-g-MAH helps to decrease the particle size. It is also noticed that in the authors' previous work,[36] the particle size distribution curves of co-powders show double peaks. However, in this work there is only one peak. The difference could be related to the different loading of WF fillers used (80 wt % in the previous work versus 60 wt % in this work).

SEM Analysis. Figure 2 shows the SEM photos of WF with different milling cycles. The pulverization process of WF under the shear force field of pan milling can be clearly observed [from Figure 2(a–d)]. The unmilled WF presents a pillar structure with aspect ratio of about 2.5. With increase of milling cycles, the WF particles are first squeezed to form flakes. Then, under the very strong three-dimensional shear force field of pan milling, the flake WF particles are split into many fiber-like pieces. Figure 2(d) clearly shows that there is a crack being formed in a fiber WF particle, along which the daughter fiber wood particles could be produced. The crack formed is the result of the stress field of pan milling. It is also noticed that while the big pillar WF particles are lengthwise cut into small fiber particles, their length is also reduced from about 530 μm to 200 μm. However, the aspect ratio of the small fiber WF particle does not decrease but increases from about 2.5 to 4.5. This reveals that the milled WF particles could have a better reinforcing effect in enhancing the mechanical properties of polymer materials.

Figure 3 shows the SEM photos of PP/WF (WPC0) and PP/WF/PP-g-MAH (WPC5) co-powders prepared at different milling cycles. From these morphology images, the mixing of the

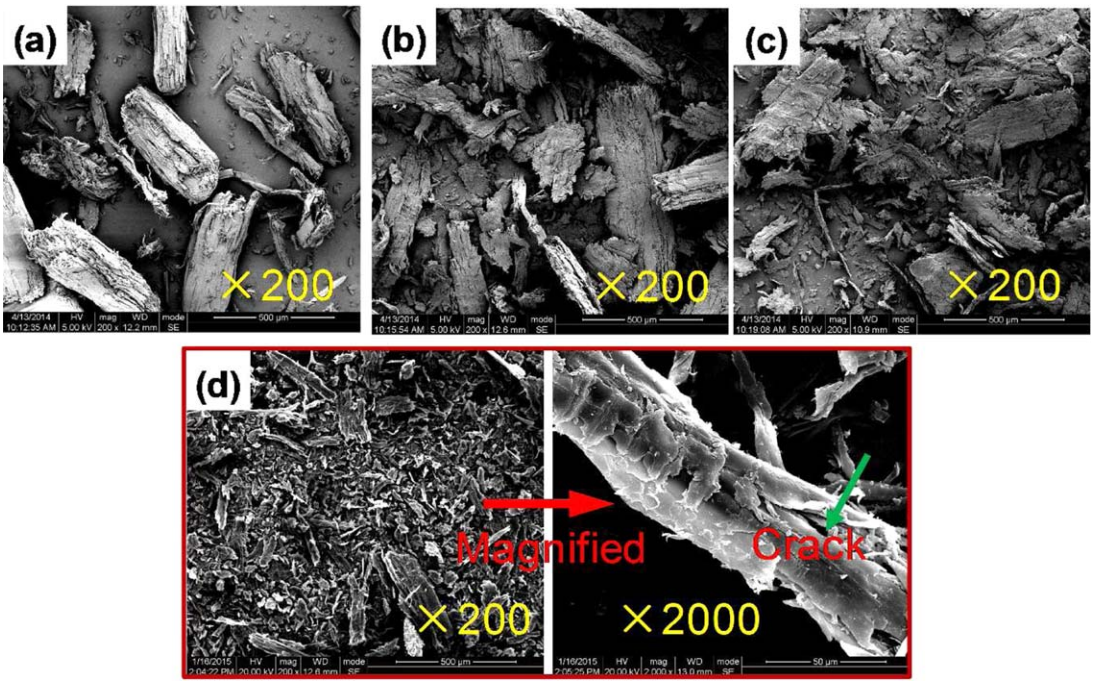

Figure 2. SEM photos of pure wood flour with different milling cycles: (a) 0, (b) 5, (c) 10, and (d) 20. [Color figure can be viewed in the online issue, which is available at wileyonlinelibrary.com.]

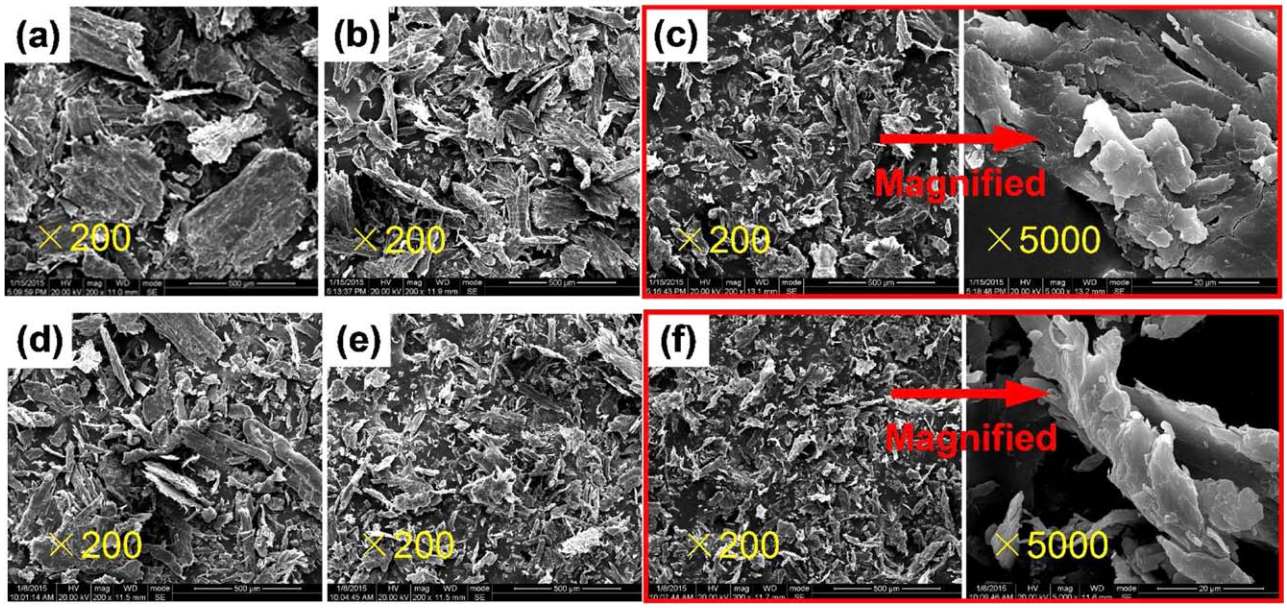

Figure 3. SEM photos of WPC0 (a–c) and WPC5 (d–f) co-powders with different milling cycles: (a) and (d) 5, (b) and (e) 10, and (c) and (f) 20. [Color figure can be viewed in the online issue, which is available at wileyonlinelibrary.com.]

pulverized WF and polymer particles and their combination can be clearly observed. The size range of the co-powder particle is in agreement with the result of the particle size analysis (Figure 1). For both systems, under the very strong shear stress field of pan milling, the mixture of WF and polymer can be equally effectively pulverized and the well mixed co-powder can be obtained. With increase of the milling cycles, the particle size of the co-powder continuously significantly decreases.

Comparing Figures 2 and 3 (especially the image with 20 milling cycles), it is noticed that the length of the fiber co-powder particle is larger than that of the milled pure WF particle. This is also a reason why the PP/WF and PP/WF/PP-g-MAH co-powders show a bigger particle size than the pure WF in the particle size measurement. Figure 3 also further verifies that the addition of PP-g-MAH could assuredly obviously decrease the dimension of the milled co-powder particle [based on the comparison between (a) and (d), (b) and (e), and (c) and (f), respectively]. The SEM images of the co-powder particles are magnified 5000 times, and it can be clearly seen that the milled co-powder particle is really the complex aggregate consisting of polymer and wood particle. The polymer particles firmly adhere to the surface of wood particles and comparatively, for PP-g-MAH contained co-powder [(d)–(f)], there are more amount of polymer particles coating and the interfacial combination is much better.

FT-IR Analysis

FT-IR spectra of pure WF with different milling cycles are shown in Figure 4(a). As can be seen, the absorption peaks occurring in the range of 3000–3750 cm^{-1} could be ascribed to the stretching vibration absorption of O–H bonds in the associated alcohol hydroxyl groups. The absorptions in the range of 600–670 cm^{-1} are caused by the out-of-plane deformation vibration of the O–H bonds. This means that there are a large number of hydrogen bonds existing in the lignocellulose. After pan milling, the absorption peaks at 3423 cm^{-1} and 666 cm^{-1} both shift toward the lower wavenumber direction, indicating that pan milling leads to the enhancement in the hydrogen bonding in system. According to the subsequent analysis, it is known that this is because pan milling makes more number of hydrogen bonds inside WF particles fully exposed, which is beneficial to the infrared detection. On the other hand, for the unmilled WF, the peak at 1510 cm^{-1} is caused by the vibration absorption of the aromatic nucleus. The absorptions at 1740 cm^{-1} and 1650 cm^{-1} are due to the stretching vibrations of the unconjugated and conjugated carbonyl groups, respectively. The occurrence of above absorptions shows that there are the possible structures of carbonyl groups connected to the benzene ring in the unmilled WF. It is noticed that, compared with unmilled WF, for the milled WF and with increasing milling cycles, the intensities of all the absorption peaks above mentioned increase and near 1600 cm^{-1} there is a new weak absorption peak occurring, which is due to the stretching vibration of aromatic nucleus. This indicates that the effect of pan milling promotes the occurrence of the carbonyl groups connected to the benzene ring. In addition, the absorption bands appearing in the range of 1050–1250 cm^{-1} are ascribed to the asymmetrical stretching vibration of C–O–C bonds. These are the characteristic absorption peaks of ether or acetal linkages, which are corresponding to the C–O–C–O–C acetal groups in the pyranoid ring of cellulose and hemicellulose in WF (before pan milling only at 1060 cm^{-1} appears a strong absorption). The influence of pan milling on the infrared absorption of WF can be explained as follows: the presence of unmilled big lignocellulose aggregates possibly negatively influences the infrared detection of the featured functional groups. However, the pan milling could cause the full exposure of the featured functional groups of lignocellulose through pulverization of WF and this

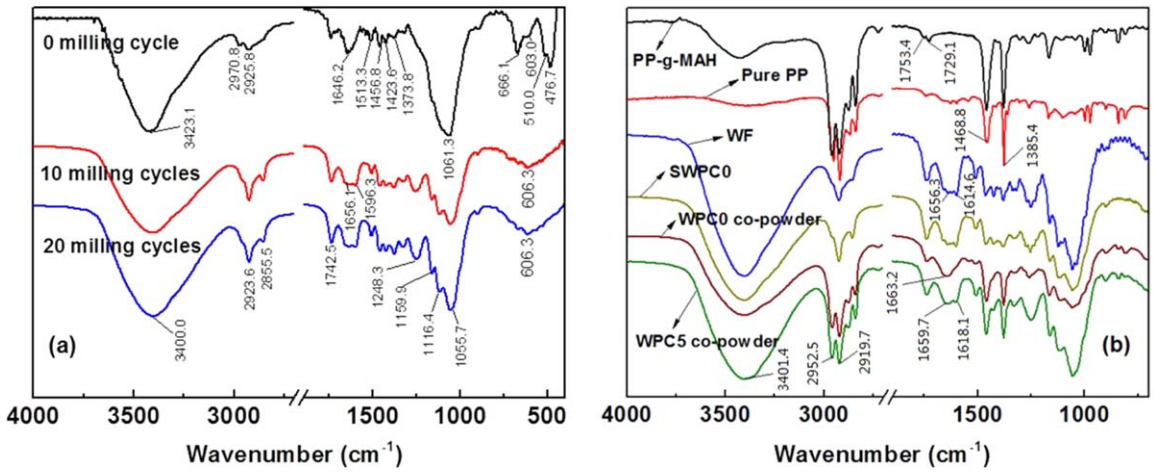

Figure 4. FT-IR spectra of different samples: (a) pure wood flour with different milling cycles and (b) pure PP, PP-g-MAH, pure wood flour milled, SWPC0, WPC0, and WPC5 co-powders (SWPC0 is the simple mixture of milled PP powder with milled wood flour; the wood flour, PP, WPC0, and WPC5 are all milled for 20 cycles). SWPC0, WPC0, and WPC5 co-powders were extracted with the boiling xylene to remove the physically adsorbed PP and PP-g-MAH for 72 h. [Color figure can be viewed in the online issue, which is available at wileyonlinelibrary.com.]

obviously would enhance the infrared absorption. This simultaneously indicates that pan milling could have an effect of activation on the lignocellulose, which is beneficial to the interfacial mechanochemical reaction.

As is seen from Figure 4(b), at 1385 and 1468 cm^{-1} are the featured absorptions of pure PP and PP-g-MAH (the bending vibration of $–CH_2–$ and $–CH_3–$ groups) and at 1729 cm^{-1} is the featured absorption of grafted MAH. For the co-powder WPC0 and WPC5, after the 72 h Soxhlet extraction there are still the stronger featured absorption peaks of PP and PP-g-MAH appearing at 1385 and 1468 cm^{-1}, indicating that under the effect of pan milling, there are the strong interactions between PP (or PP-g-MAH) and lignocellulose. For WPC5, such a strong interaction could be regarded as the chemical bonding which is formed through the mechanochemical grafting esterification reaction of PP-g-MAH with –OH groups at the surface of WF particles under the effect of pan milling.[36] This is because except for existence of the featured absorptions of the left polymer after extraction, there are the bands occurring in the range of 1610–1660 cm^{-1}, which have a profile similar to that of the authors' previous work.[36] The peak at 1660 cm^{-1} is assigned to the absorption of C=O in ester group [this peak should have appeared at a higher wavenumber (>1660 cm^{-1}), but actually it exhibits a red shift (moves toward lower wavenumber direction) due to formation of the possible intramolecular hydrogen bonding between the formed ester group and the nearby carboxyl group]. The formation mechanism of the graft reaction product of PP-g-MAH with lignocellulose can be illustrated using Figure 5(2). For WPC0, the strong interaction above mentioned could be also identified as chemical bonding rather than physical adsorption, which is based on the following consideration. In this experiment, the WPC0 sample was Soxhlet-extracted using boiling xylene for 72 h to remove the physically adsorbed PP macromolecular chains. If the physically adsorbed PP macromolecular chains are completely removed, the left PP macromolecular chains [indicated by Figure 4(b)] can be believed to be chemically bonded onto the surface of WF particles. In order to prove this, the simple mixture of milled WF powders (60 wt %) and milled PP powders (SWPC0) (before mixing, WF particles and PP pellets were separately milled for 20 cycles. Then, the milled WF powders and the milled PP powders were adequately mixed in a high speed mixer) was also Soxhlet-extracted for 72 h using the boiling xylene. The extracted SWPC0 sample was analyzed by using FT-IR spectrometer too. The result is shown in Figure 4(b) (SWPC0). As can be seen, the FT-IR spectrum of the extracted SWPC0 is more like that of milled WF and the featured absorptions of PP (1468 and 1385 cm^{-1}) have disappeared. This indicates that the milled PP powders in the simple mixture, which are physically adsorbed on the surface of WF particles, are almost completely removed by using the boiling xylene. That is to say, in the extracted WPC0, the physically adsorbed PP macromolecular chains have been almost completely removed and the left PP macromolecular chains prove to be chemically bonded onto the surface of WF particles. The grafting mechanism of PP with lignocellulose is shown in Figure 5(1). Under the very strong shear stress field of pan milling, the C–C bonds on PP backbone macromolecular chains and the C–O bonds between the pyranoid rings on lignocellulose backbone macromolecular chains would be broken to generate the corresponding macromolecular radicals.[31,38,39] The macromolecular radicals of PP and WF lignocellulose would combine instantly to form the PP-WF grafting products. Comparing the intensity of absorption peaks between WPC0 and WPC5, it is seen that the grafting efficiency of PP-g-MAH with lignocellulose is higher than that of PP with lignocellulose.

Preparation and Characterization of PP/WF Composites

Morphological Analysis. The prepared PP/WF co-powders with and without PP-g-MAH were extruded and injection molded into various specimen for test. Figure 6 shows the SEM photos of the fractured cross-section of WPC0 sample without compatibilizer PP-g-MAH. As can be clearly seen, for the unmilled sample, both the dispersion of WF particles and the compatibility are very poor. There are many big WF aggregates with poor

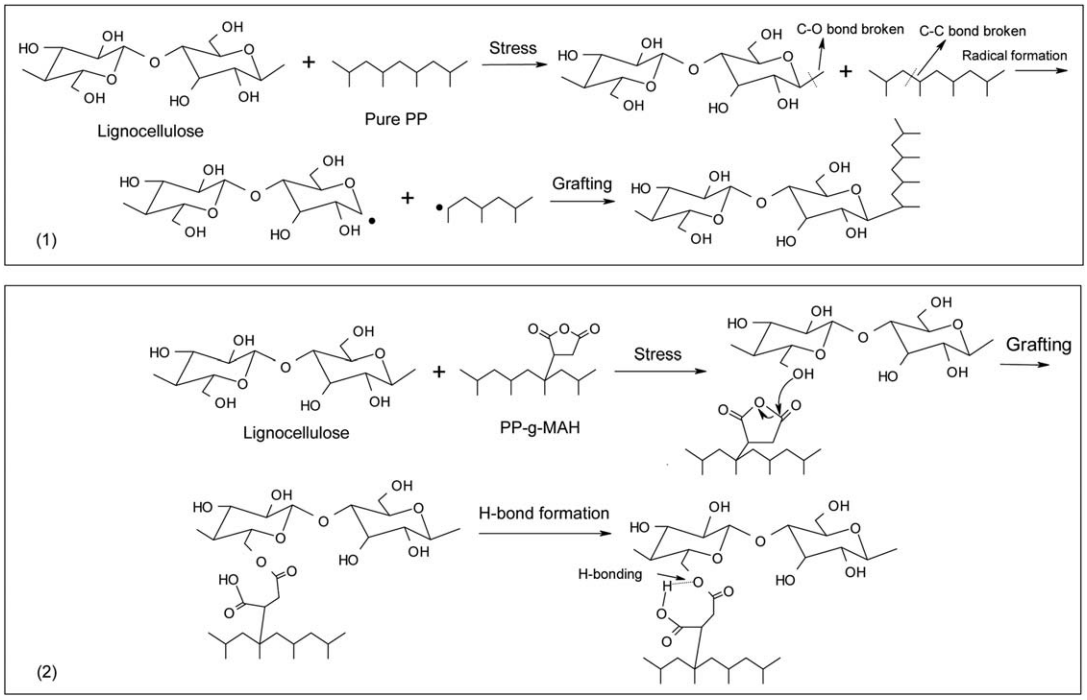

Figure 5. The mechanochemical graft reaction of pure PP or PP-g-MAH with lignocellulose under the effect of pan milling.

interfacial bonding (obvious gap at the filler–matrix interface) present in PP matrix [Figure 6(a,d)]. With increase of milling cycles, the dispersion of WF particles and the interfacial combination in system become better and better. There are many fiber WF particles with reduced radial size evenly distributed in PP matrix. With increasing the milling cycle to 20, the dispersion of the fiber WF particles and the interfacial bonding between filler and PP matrix have been substantially improved.

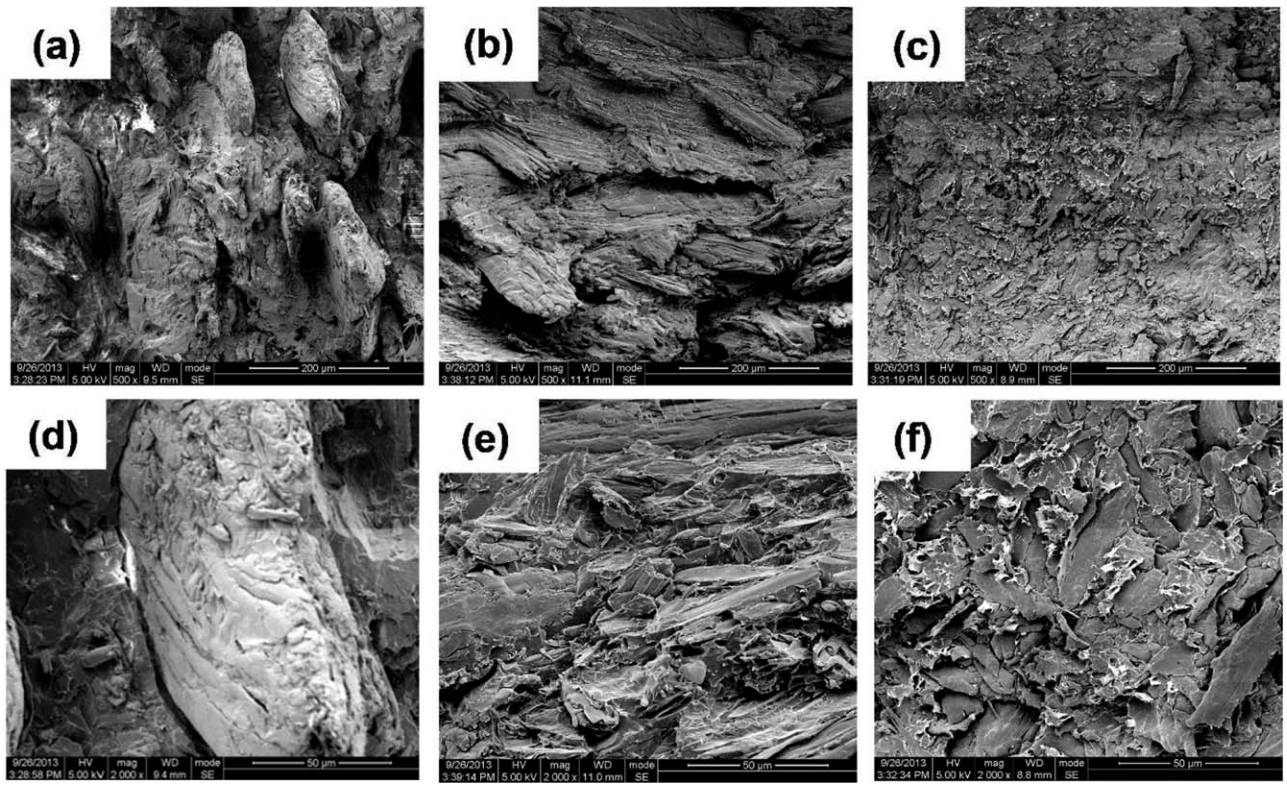

Figure 6. SEM photos of the fractured surface of WPC0 composites prepared at different milling cycles: (a) and (d) 0, (b) and (e) 5, and (c) and (f) 20. Images (a)–(c) are in 500 magnification and images (d)–(f) are in 2000 magnification.

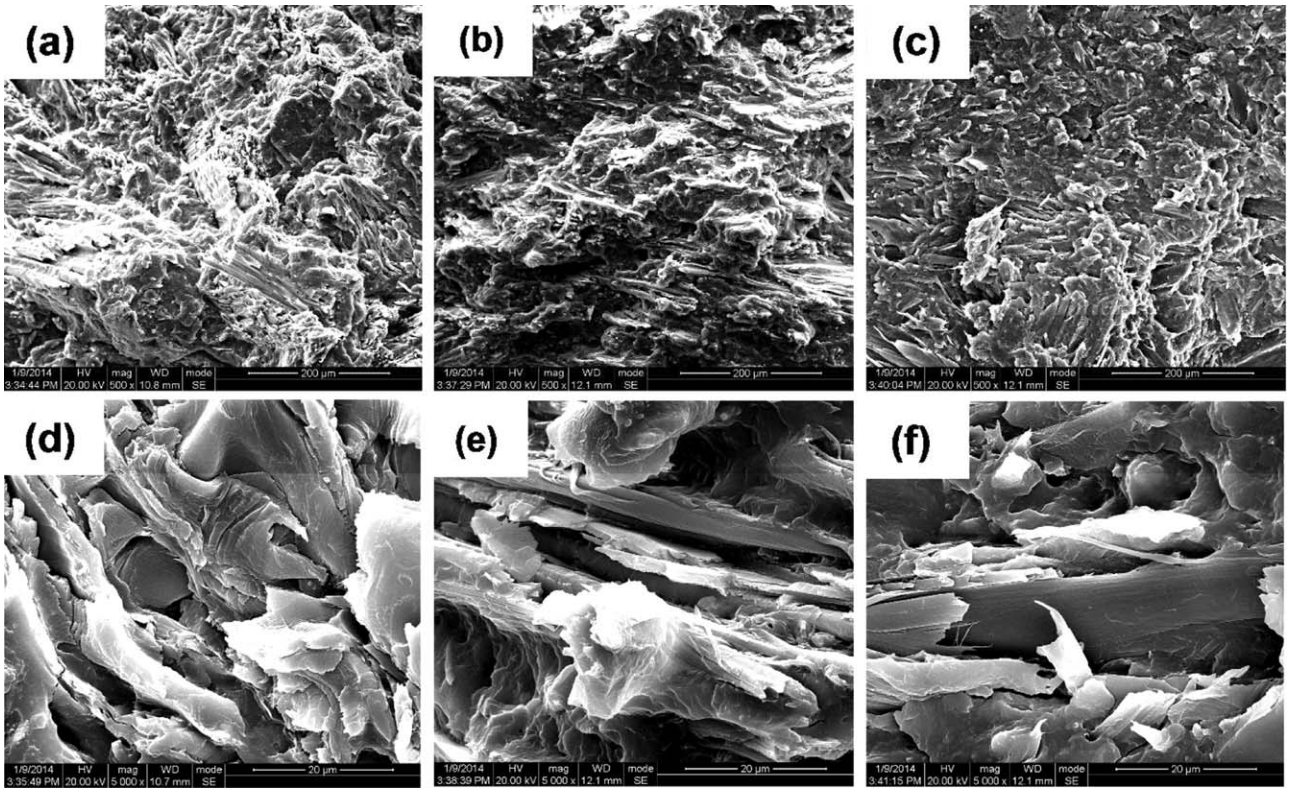

Figure 7. SEM photos of the fractured surface of WPC5 composites prepared at different milling cycles: (a) and (d) 0, (b) and (e), 5 and (c) and (f) 20. Images (a)–(c) are in 500 magnification and images (d)–(f) are in 5000 magnification.

Figure 7 shows the SEM photos of the fractured cross-section of WPC5 sample with 5 wt % compatibilizer PP-g-MAH. As can be seen, compared with the uncompatibilized WPC0 system [Figure 6(a,d)], the dispersion of WF particles and the compatibility in PP-g-MAH compatibilized WPC5 system are greatly improved. Particularly, the dimension of the WF particles is effectively reduced possibly due to the co-effect of PP-g-MAH and shearing force field of extruder. However, the small interfacial gap between WF filler and matrix can be still observed [Figure 7(d)]. For the milled WPC5 system, the pan-milling effect further substantially ameliorates the dispersion of the fiber WF particles and the interfacial combination. Under the effect of pan milling, the size of the WF particles is remarkably reduced and the big aspect ratio can still be maintained. Meanwhile, there are almost no interfacial gaps observed at the interface. With increase of milling cycles to 20, the homogeneously dispersed WF particles and the excellent interfacial bonding have been realized in PP matrix, which results from the strong pulverization, dispersion and mixing functions of pan mill and also its mechanochemical compatibilization effect (Figure 5). This would obviously be advantageous to the great enhancement in the mechanical performance.

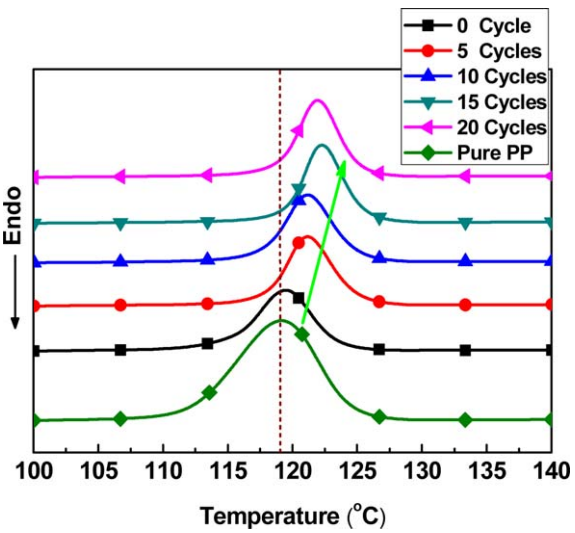

Figure 8. The DSC cooling curves of pure PP and WPC0 composites prepared at different milling cycles. [Color figure can be viewed in the online issue, which is available at wileyonlinelibrary.com.]

Thermal Analysis. The nonisothermal crystallization behavior of WPC0 system was investigated, as shown in Figure 8. The corresponding crystallization parameters are included in Table III. It is seen that, relative to pure PP, the addition of WF particles (for unmilled WPC0 system) increases the initial crystallization temperature and the crystallization temperature of PP slightly. This indicates that the incorporated WF particles have a heterogeneous nucleation effect on the crystallization of PP to a certain degree. In addition, it is noticed that the pan milling shows an obvious influence on the crystallization of PP. From Figure 8 and Table III, it is clearly seen that with increase of milling cycles, the initial crystallization temperature and the crystallization temperature of WPC0 sample obviously shift

Table III. Nonisothermal Crystallization Parameters of Pure PP and WPC0 Composites Prepared at Different Milling Cycles

Milling cycles	H_c (J g^{-1})	T_{c0} (°C)	T_c (°C)	ΔT_c (°C)	X_c
0	37.5	105.0	119.5	22.6	31.1%
5	37.9	108.8	121.3	21.7	33.3%
10	38.1	110.1	121.6	19.4	34.9%
15	37.5	110.3	122.6	19.2	37.9%
20	37.8	109.8	122.3	19.2	38.1%
Pure PP	85.3	103.3	119.1	26.3	36.9%

Note: H_c, T_{c0}, T_c, ΔT_c, and X_c are crystallization enthalpy, initial crystallization temperature, crystallization temperature, the difference between crystallization temperature and initial crystallization temperature and crystallinity, respectively.

toward the high temperature direction. The increase does not cease until the milling cycles exceed 15. This shows that pan milling could remarkably enhance the heterogeneous nucleation effect of WF particles on the crystallization of PP macromolecular chains. The essential reason for this is that pan milling is beneficial to the remarkable improvement in the dispersion of WF fillers. The WF particles with greatly improved dispersion in PP matrix can of course have the significantly enhanced heterogeneous nucleation capability. When the milling cycles exceed 15, the heterogeneous nucleation effects of WF fillers decrease. This is because the excessive milling would possibly cause the deterioration in the dispersion of WF fillers to a certain degree. From Table III, it is also seen that the crystallinity of the unmilled WPC0 sample is obviously lower than that of pure PP. This indicates that although the WF fillers have the heterogeneous nucleation effect on PP crystallization, the high loading of the heavily agglomerated WF particles [Figure 6(a,d)] are still disadvantageous to the crystallization of PP macromolecular chains to a great extent, leading to obvious decrease in crystallinity. With increase of milling cycles, the crystallinity of unmilled WPC0 shows an obviously increasing tendency and even surpasses that of pure PP at milling cycles of 15. Similarly, this could be ascribed to the great improvement in dispersion of WF particles resulted from the effect of pan milling. The WF particles with better dispersion could play the better heterogeneous nucleation role in promoting the PP crystallization.

In order to investigate the dynamic mechanical properties of WPC material, the DMA were carried out. Figure 9 shows the storage modulus (E'), loss modulus (E''), and mechanical loss factor (tanδ) of WPC samples with and without PP-g-MAH as

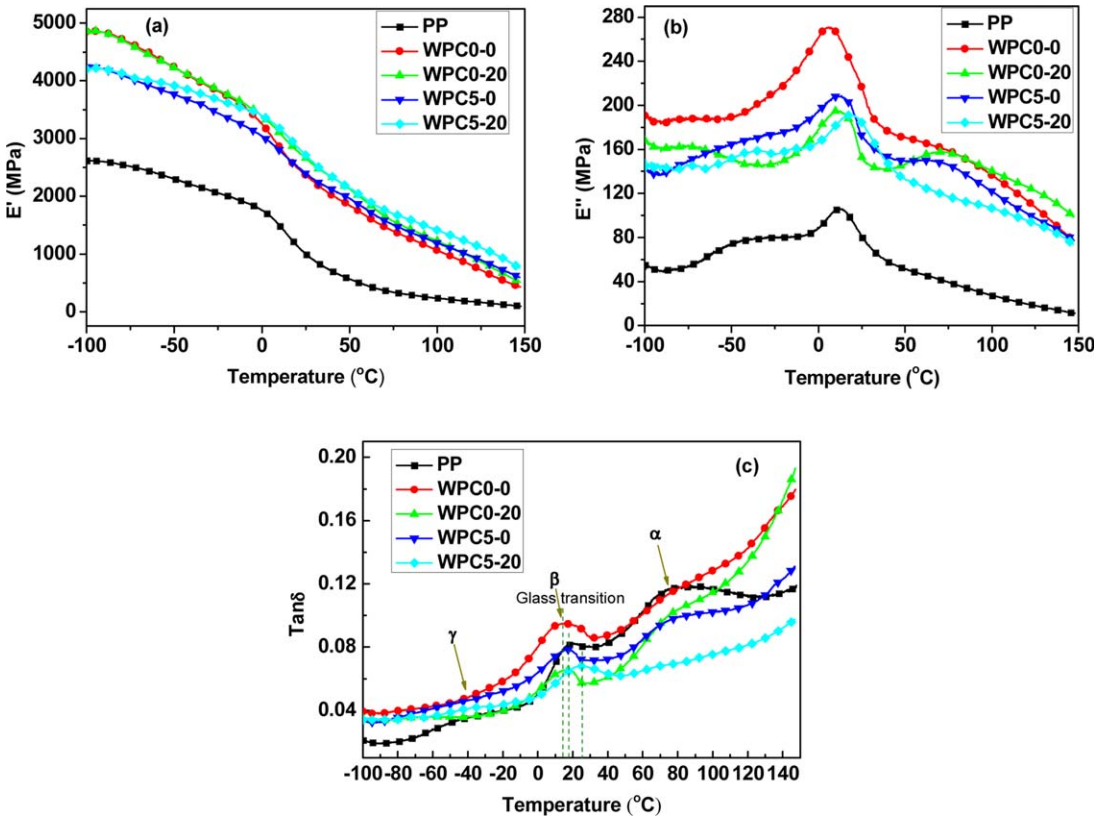

Figure 9. Temperature dependence of (a) storage modulus E', (b) loss modulus E'' and (c) tanδ of pure PP and WPC samples (WPC0-0 means without milling and PP-g-MAH, WPC 0-20 means without PP-g-MAH and with 20 milling cycles, WPC5-0 means with 5 wt % PP-g-MAH and without milling, and WPC5-20 means with 5 wt % PP-g-MAH and 20 milling cycles). [Color figure can be viewed in the online issue, which is available at wileyonlinelibrary.com.]

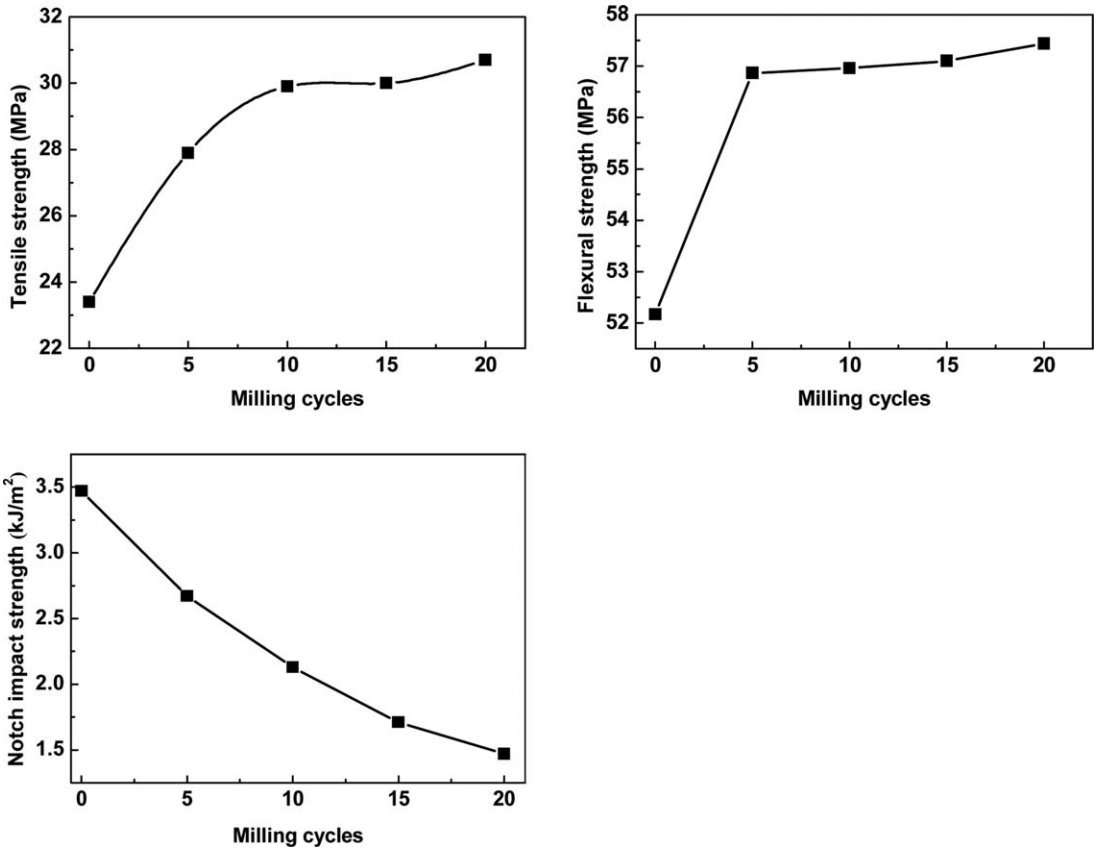

Figure 10. Effect of milling cycle on the mechanical performance of WPC0 composite.

a function of temperature from −100°C to 150°C. For the evolution of E' with temperature [Figure 9(a)], E' always presents a declining tendency with increase in temperature. This could be ascribed to the increased mobility of molecular segments upon heating, resulting in decrease in stiffness. Relative to pure PP, the composite systems always show a much higher E' value. This is because the incorporated WF fillers impart a big reinforcement to PP, which can make the stress transfer from the matrix to the reinforcing wood fibers.[40] It is noticed that both pan milling and addition of PP-g-MAH compatibilizer have influence on E' value. However, the influence of PP-g-MAH in the different temperature range is different. At low temperature (<-20°C), the E' values of the milled sample and unmilled sample are similar. However, the E' values of samples with PP-g-MAH are obviously lower than those of samples without PP-g-MAH. This is possibly related to the plasticization effect of PP-g-MAH behaving at low temperature. On the contrary, at high temperature (>0°C), the case is different. The incorporation of PP-g-MAH can slightly increase the E' value due to the enhanced interfacial interaction through introduction of compatibilizer. In addition, the pan-milling is found to be able to increase the E' value of PP/WF composite (WPC0-0 versus WPC0-20). This is because pan milling induces the grafting of PP macromolecular chains onto the surface of WF particles, as evidenced by FT-IR spectra. On the other hand, for PP-g-MAH incorporated system, the pan milling similarly further obviously enhances the E' value of composite (WPC5-0 versus WPC5-20), which could be ascribed to such a fact that the pan milling promotes the grafting reaction of PP-g-MAH with lignocellulose and further enhances the interfacial bonding. Above results again prove the functions of stress induced mechanochemical reaction of pan-mill equipment in turn.

For the evolution of E'' with temperature [Figure 9(b)], all samples show a loss modulus peak at about 10°C, which corresponds to the glass transition. This will be next analyzed by combining the tanδ spectra shown in Figure 9(c). It is also noticed that all composites present a much higher E'' value than pure PP. The reason for this is mainly due to the formation of the interface between PP matrix and the rigid WF filler particles.[41] Under the effect of the external field (shear force field during extrusion or injection molding), the interfacial frictions between PP macromolecular chains and the much stiffer WF particles generated due to their relative motion are much stronger than the intermolecular frictions between PP macromolecular chains themselves, leading to the energy dissipation of the former being higher than that of the latter. Also, it is interestingly noticed that the unmilled WPC0 sample without PP-g-MAH has an obviously higher E'' value than the other samples. This is because the unmilled and uncompatibilized WPC0 sample has the poorest interfacial bonding, hence leading to the strongest interfacial frictions. Compared with the unmilled WPC0 sample, the milled WPC0 sample shows the remarkably decreased E'' value. The reason for this is similarly due to formation of the greatly enhanced interfacial combination through graft of PP molecular chains onto the surface of

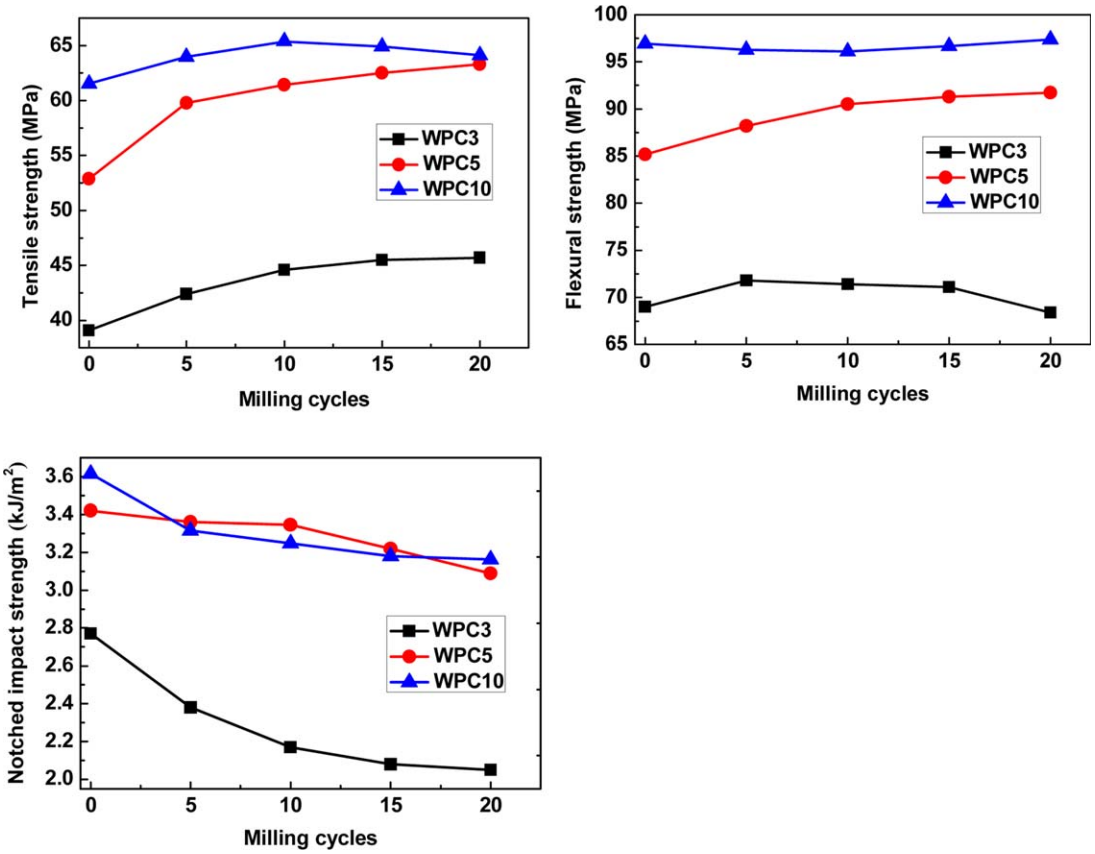

Figure 11. Effect of milling cycle on the mechanical performance of PP/WF composite with different content of PP-g-MAH. [Color figure can be viewed in the online issue, which is available at wileyonlinelibrary.com.]

WF particles under the effect of pan milling. On the other hand, the incorporation of compatibilizer also obviously reduces the E'' value (WPC0-0 versus WPC5-0) and this is also due to the improvement in the interfacial compatibility. Comparing WPC5-0 with WPC5-20, it is clear that the pan milling further decreases the E'' value of sample. The reason for this could be also that pan milling further improves the interfacial bonding through promoting the graft reaction of the added PP-g-MAH with WF particles.

For the evolution of tanδ with temperature [Figure 9(c)], in the tanδ curve of pure PP, there are three peaks identified at -36.3°C, 17.5°C, and 77.5°C, which correspond to γ transition, β transition, and α transition of PP, respectively. The γ transition (also γ relaxation) at -36.3°C is caused by the local segmental motion at atomic level in amorphous region of PP (e.g., the inner-revolving motion of α-methyl groups attached to the backbone chains).[42] The β transition at 17.5°C is the dominant relaxation form (damping) of PP, which is generally regarded as the glass transition of PP (change from rigid to rubbery state) and it is caused by the relaxation motions of amorphous PP chain segments. The α transition at 77.5°C is caused by the slips of crystal lamellae and the relaxations of the restricted amorphous chain segments in crystals.[43] It is often related to the imperfections in the crystalline region. As is seen from Figure 9(c), the T_g of unmilled WPC0 sample (14.4°C) decreases relative to that of pure PP (17.5°C). This is an interesting phenomenon. It can be illustrated with the aid of the DSC results discussed before (Figure 8). The added WF particles are the nucleating agents for PP crystallization and they would accelerate the crystallization of PP macromolecular chains. Such a crystallization acceleration process would make the amorphous PP chain segments have more mobility[44] in composite, leading to the decrease in T_g of PP. Another possible reason is related to the fragments sheared off the wood fibers during melt processing, which possibly act as the plasticizer.[45] It is also seen that the combination of pan milling and PP-g-MAH effectively improves the T_g of PP, e.g., for WPC5-20 sample, its T_g (25°C) is obviously higher than that of pure PP. This is because both pan milling and the added PP-g-MAH substantially enhance the interfacial bonding (interaction) and hence greatly decrease the mobility of PP amorphous chain segments. It is noticed in Figure 9 that from sample WPC0-0 to WPC5-20, the damping (tanδ peak) at glass transition is gradually weakened. This is also related to the decrease in the number of the free amorphous phase in composite, because pan milling or incorporation of interfacial modifier PP-g-MAH can equally enhance the interfacial interaction and hence lead to the restriction of molecular chain segments motion. In addition, the WPC5-20 sample shows the lowest α transition peak intensity, indicating that this milled and compatibilized system has the fewest deficiencies in crystalline phase.

Mechanical Properties. Figure 10 shows the influence of milling cycles on the mechanical performance of WPC0 materials. It

can be seen that pan milling can obviously improve the tensile strength and flexural strength of PP/WF composites. With increasing milling cycles from 0 to 20, the tensile strength and flexural strength increase from 23.5 to 30.8 MPa (31% higher) and from 52.2 to 57.5 MPa (10% higher), respectively. However, the notched impact strength shows an obviously decreasing tendency. The reasons for the improvement in tensile and flexural performance of the composite could be attributed to the improved dispersion of WF fillers and the enhanced interfacial performance between WF and PP matrix, induced by the pan-milling effect. The decrease in the impact strength of composite may be due to the possible degradation of PP matrix during pan milling.

Figure 11 shows the influence of pan milling and the added PP-g-MAH on the mechanical performance of PP/WF composites. It can be seen that the addition of compatibilizer PP-g-MAH substantially enhances the mechanical properties of composite (compared with Figure 10), especially for tensile strength and flexural strength. With increase in PP-g-MAH content, almost all mechanical properties increase a lot (especially from 0 to 3 wt % and from 3 to 5 wt %). However, the excessive increase of PP-g-MAH content would not lead to an obvious increase in mechanical properties. The great improvement caused by PP-g-MAH could be attributed to its good compatibilizing role. Totally, the pan milling was found to have a positive influence on the mechanical performance of composite with PP-g-MAH, particularly for tensile strength and flexural strength. Generally, at low PP-g-MAH content, the influence is big and at high PP-g-MAH content, the influence is small. Comparatively, with increasing milling cycles, the tensile strength increases more obviously; the flexural strength increases slowly; the notched impact strength still shows a decreasing tendency and, however, the decrease degree is much smaller relative to the composite without PP-g-MAH. The reason for the amelioration effect could be that pan milling further enhances the interfacial bonding through promoting the graft reaction of PP-g-MAH with wood fibers. When 10 wt % PP-g-MAH and 10 milling cycles are used, the prepared PP/WF composite possesses the best comprehensive performance, achieving tensile strength of 65.1 MPa, flexural strength of 95.2 MPa, and notched impact strength of 3.3 kJ/m^2. The mechanical performance of the PP/WF composite prepared in this work can be comparable with that of 80 wt % WF fillers incorporated PP composite reported in the authors' previous work.[36] This sufficiently shows the advantages of the self-designed pan-mill equipment in the authors' laboratory in preparation of highly filled WPC.

CONCLUSIONS

Solid-state shear milling (S^{3}M) method was used to prepare PP/WF co-powders and the corresponding composites with high performances. The pulverization, crystallization, structure, and property of PP/WF system were accordingly investigated in detail. Under the effect of the strong three-dimensional shear force field generated by pan milling, the mixture of PP and WF particles is effectively pulverized and the well-mixed PP/WF mixture could be obtained. After pulverization, the aspect ratio of the obtained WF particles does not decrease but increases instead. The pan milling causes the closer combination of WF particles with PP polymer and even realizes the coating of a part of polymer particles on the surface of WF particles. The incorporation of PP-g-MAH is found to be helpful to the size reduction of PP/WF mixture. In addition, the strong shear force field of pan milling could adequately activate the WF fillers by exposure of their characteristic functional groups (e.g., hydroxyl groups, carbonyl groups, etc.). The pan milling could also realize the grafting of the macromolecular chains of both PP and PP-g-MAH onto the surface of WF particles. As a result, the interfacial compatibility between WF fillers and PP matrix could be remarkably improved by combining pan milling and the incorporation of PP-g-MAH, as evidenced by SEM characterization. Correspondingly, both the storage modulus and the glass transition temperature of the milled and compatibilized PP/WF composites are obviously increased. Also, the added WF particles show the heterogeneous nucleation effect on PP crystallization, which can be remarkably enhanced by the combination of pan milling. The prepared PP/WF composite possesses an excellent comprehensive performance and shows good application prospects.

ACKNOWLEDGMENTS

This work was supported by the National Natural Science Foundation of China (51421061 and 51433006), National High Technology Research and Development Program (863 Program, 2012AA063003), and the Program of Introducing Talents of Discipline to Universities (B13040).

REFERENCES

1. Tronc, E.; Hernandez-Escobar, C. A.; Ibarra-Gomez, R.; Estrada-Monje, A.; Navarrete-Bolaños, J.; Zaragoza-Contreras, E. A. *Carbohydr. Polym.* **2007**, *67*, 245.
2. Thakur, V. K.; Thakur, M. K.; Gupta, R. K. *Int. J. Polym. Anal. Chem.* **2014**, *19*, 256.
3. Karmarkar, A.; Chauhan, S. S.; Modak, J. M.; Chanda, M. *Composites Part A* **2007**, *38*, 227.
4. Jawaid, M.; Khalil, H. P. S. A. *Carbohydr. Polym.* **2011**, *86*, 1.
5. Thakur, V. K.; Thakur, M. K.; Gupta, R. K. *Carbohydr. Polym.* **2014**, *104*, 87.
6. Thakur, V. K.; Singha, A. S.; Thakur, M. K. *Int. J. Polym. Mater.* **2013**, *62*, 226.
7. Sanadi, A. R.; Caulfield, D. F.; Jacobson, R. E.; Rowell, R. M. *Ind. Eng. Chem. Res.* **1995**, *34*, 1889.
8. Părpăriţă, E.; Darie, R. N.; Popescu, C. M.; Uddin, M. A.; Vasile, C. *Mater. Des.* **2014**, *56*, 763.
9. Huda, M. S.; Drzal, L. T.; Misra, M. *Ind. Eng. Chem. Res.* **2005**, *44*, 5593.
10. George, J.; Sreekala, M. S.; Thomas, S. *Polym. Eng. Sci.* **2001**, *41*, 1471.
11. Lei, Y.; Wu, Q. *Bioresour. Technol.* **2010**, *101*, 3665.
12. Takatani, M.; Ikeda, K.; Sakamoto, K.; Okamoto, T. *J. Wood Sci.* **2008**, *54*, 54.

13. Lai, S. M.; Yeh, F. C.; Wang, Y.; Chan, H. C.; Shen, H. F. *J Appl. Polym. Sci.* **2003**, *87*, 487.
14. Rozman, H. D.; Tan, K. W.; Kumar, R. N.; Abubakar, A.; Ishak, Z. A. M.; Ismail, H. *Eur. Polym. J.* **2000**, *36*, 1483.
15. Bledzki, A. K.; Mamun, A. A.; Jaszkiewicz, A.; Erdmann, K. *Compos. Sci. Technol.* **2010**, *70*, 854.
16. Maldas, D.; Kokta, B. V. *Polym. J.* **1991**, *23*, 1163.
17. Tabari, H. Z.; Nourbakhsh, A.; Ashori, A. *Polym. Eng. Sci.* **2011**, *51*, 272.
18. Ly, B.; Thielemans, W.; Dufresne, A.; Chaussy, D.; Belgacem, M. N. *Compos. Sci. Technol.* **2008**, *68*, 3193.
19. Qiu, W.; Mai, K.; Zeng, H. *J. Appl. Polym. Sci.* **2000**, *77*, 2974.
20. Lee, S. Y.; Yang, H. S.; Kim, H. J.; Jeong, C. S.; Lim, B. S.; Lee, J. N. *Compos. Struct.* **2004**, *65*, 459.
21. Bledzki, A. K.; Reihmane, S.; Gassan, J. *J. Appl. Polym. Sci.* **1996**, *59*, 1329.
22. Pickering, K. L.; Beckermann, G. W.; Alam, S. N.; Foreman, N. *J. Compos. Part A* **2007**, *38*, 461.
23. Rahman, M. M. *Mater. Des.* **2009**, *30*, 2191.
24. Gomes, A.; Matsuo, T.; Goda, K.; Ohgi, J. *Compos. Part A* **2007**, *38*, 1811.
25. Woodhams, R. T.; Thomas, G.; Rodgers, D. K. *Polym. Eng. Sci.* **1984**, *24*, 1166.
26. Maiti, S. N.; Hassan, M. R. *J. Appl. Polym. Sci.* **1989**, *37*, 2019.
27. Shukla, S. R.; Rao, G. V.; Athalye, A. R. *J. Appl. Polym. Sci.* **1991**, *42*, 2163.
28. Thakur, V. K.; Thakur, M. K.; Gupta, R. K. *Carbohydr. Polym.* **2013**, *97*, 18.
29. Canché-Escamilla, G.; Rodriguez-Laviada, J.; Cauich-Cupul, J. I.; Mendizábal, E.; Puig, J. E.; Herrera-Franco, P. *J. Compos. Part A* **2002**, *33*, 539.
30. Xu, X.; Wang, Q. CN Patent ZL95111258.9, **1995**.
31. Liu, C.; Wang, Q. *J. Appl. Polym. Sci.* **2000**, *78*, 2191.
32. Chen, Z.; Wang, Q. *Polym. Int.* **2001**, *50*, 966.
33. Wang, B.; Wang, Q.; Li, L. *J. Macromol. Sci. Part B: Phys.* **2014**, *53*, 78.
34. Lu, C.; Wang, Q. *J Mater. Proces. Technol.* **2004**, *145*, 336.
35. Shao, W.; Wang, Q.; Wang, F.; Chen, Y. *Carbon* **2006**, *44*, 2708.
36. Niu, Z. H.; Chen, Y. H.; Bai, S. B. *CIESC J.* **2014**, *65*, 5039.
37. Avella, M.; dell'Erba, R.; Martuscelli, E.; Ragosta, G. *Polymer* **1993**, *34*, 2951.
38. Zhang, Y. L.; Guo, Z. F.; Zhang, L. M.; Pan, L. S.; Tian, Z.; Pang, S. J.; Xu, N.; Lin, Q. *Polym. Bull.* **2015**, *72*, 1949.
39. Voronov, A.; Kohut, A.; Synytska, A.; Peukert, W. *J. Appl. Polym. Sci.* **2007**, *104*, 3708.
40. Rana, A. K.; Mitra, B. C.; Banerjee, A. N. *J. Appl. Polym. Sci.* **1999**, *71*, 531.
41. Huda, M. S.; Drzal, L. T.; Mohanty, A. K.; Misra, M. *Compos. Part B* **2007**, *38*, 367.
42. García-Martínez, J. M.; Areso, S.; Taranco, J.; Collar, E. P. *Res. Rev. Mater. Sci. Chem.* **2014**, *4*, 35.
43. Jiru, Y.; Xie, X.; Zhou, X.; Zhou, H.; Li, D. *Chem. Res. Chin. Univ.* **2009**, *25*, 573.
44. Diez-Gutiérrez, S.; Rodriguez-Pérez, M. A.; De Saja, J. A.; Velasco, J. I. *Polymer* **1999**, *40*, 5345.
45. Tajvidi, M.; Falk, R. H.; Hermanson, J. C. *J. Appl. Polym. Sci.* **2006**, *101*, 4341.